

Comparison of fuzzy logic and neural network in maximum power point tracker for PV systems

Chokri Ben Salah*, Mohamed Ouali

Research Unit on Intelligent Control, Optimization, Design & Optimization of Complex Systems (ICOS), Department of Electrical Engineering, National School of Engineers of Sfax, BP. W, 3038, Sfax, Tunisia

ARTICLE INFO

Article history:

Received 20 March 2009
Received in revised form 27 June 2010
Accepted 5 July 2010
Available online 31 July 2010

Keywords:

Fuzzy logic
Neural network
Photovoltaic
MPPT
Simulation
Modelling

ABSTRACT

This paper proposes two methods of maximum power point tracking using a fuzzy logic and a neural network controllers for photovoltaic systems. The two maximum power point tracking controllers receive solar radiation and photovoltaic cell temperature as inputs, and estimated the optimum duty cycle corresponding to maximum power as output. The approach is validated on a 100 Wp PVP (two parallels SM50-H panel) connected to a 24 V dc load. The new method gives a good maximum power operation of any photovoltaic array under different conditions such as changing solar radiation and PV cell temperature. From the simulation and experimental results, the fuzzy logic controller can deliver more power than the neural network controller and can give more power than other different methods in literature.

© 2010 Elsevier B.V. All rights reserved.

1. Introduction

The maximum power point tracking (MPPT) is a controlled dc–dc inverter that monitors a photovoltaic panel (PVP) to operate at its maximum power point (MPP) depending on the state of load, PVP generation, photovoltaic (PV) cell temperature (T) and solar radiation (G) variations [1]. In such a direction, different techniques and algorithms have been presented. The most encountered method known as the incremental conductance is reviewed in [2]. In [3,4], an algorithm forcing the load conductance at the optimum value is provided. The duty cycle of the PWM signal that controls the dc–dc converter connected to the PVP is therefore continually adjusted depending on the load current and voltage. In [5] and [6] an MPPT using sliding mode current controller for PVP system is also proposed, yielding an algorithm principle consisting in varying the load voltage until attempting the power or the current derivative by the voltage reaches zero. Furthermore, intelligent methods as artificial neural networks (NN), genetic algorithms and fuzzy logic (FL) have been also adopted to estimate the voltage and the current values of the load. And then to vary the duty cycle of the dc–dc converter so as to place the PVP system in its MPP at any given G , T , and load conditions [7,8]. For more

details on these methods and some related applications on solar energy, PVP, etc. the riders can refer to [7–12] and the references therein.

In all cases, the proposed MPPT algorithms ensure MPP from PVP. However, since these methods determine the optimum values of load voltage and current by moving the functioning point along the I – V curve of the PVP, they cannot deliver fast decision face to climate disturbance or load fluctuation. Hence, an overall system delay is consequently observed. Many researches have estimated the MPPT by FL and by NN methods. [13,14] calculated the MPP of the PVP by the FL controller. The FL controller in [13,14] uses the outputs current I and voltage V from PV array, the calculation of the change of output current $I(k) - I(k-1)$ and the change of output voltage $V(k) - V(k-1)$, which increases the complexity of the algorithm and complicates the implementation. [15,16] estimated the MPP of the PVP by the NN methods, in these papers the determination of the MPP needed the acquisition of the weather parameters G and T which are the inputs of the NN controller to estimate the MPP, the acquisition of the outputs current and voltage of the PVP, respectively, I and V to calculate the MPP with the module power, these two estimated MPPs are the inputs of the control algorithm to calculate in its output the error of MPP which is the input of the Digital analogic converter (DA) and driving circuits to generate the duty cycle correspond to the MPP to control the dc–dc inverter. This method proposed in [15,16] needed many electronic stages to implement it, stage of data acquisition, stage of NN controller, stage of control algorithm,

* Corresponding author.

E-mail address: chokribs@yahoo.fr (C. Ben Salah).

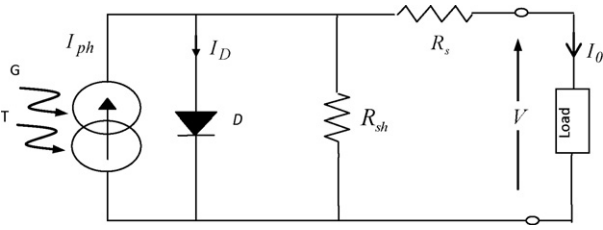


Fig. 1. Equivalent circuit of a photovoltaic cell.

and DA and driving stage. These many stages complicate the implementation of this method and present a high cost.

In order to solve this problem of complexity and high cost and to improve the stability of the MPPT controller, two MPPT controllers use a FL and NN algorithms of the PVP behaviour when functioning in its experimental conditions are proposed. These two controllers use the climatic parameters T and G in the inputs and estimated the optimum duty cycle (α_{opt}) correspond to the maximum power (P_{max}) in the outputs to control the dc–dc inverter, which gives simplicity and low cost to implement it. The FL is appropriate for non-linear control and does not use complex mathematics. Behaviours of FL depend on the shape of membership functions and rule base. There is no formal method to determine accurately the parameters of the controller. However, choosing fuzzy parameters to yield optimum operating point and a good control system depends on the experience of the designer and the measured test.

The benefits of using NN are that there is no requirement for knowledge on internal system parameters, less computational effort and they provide a compact solution for multivariable problems. Since the α_{opt} is directly obtained by using NN, the proposed method does not need complex algorithms and advanced power electronic control units.

The present paper will be organized as follows. Section 2 gives the PVP model. The system configuration, the proposed approach and the FL and NN controllers are exposed in Section 3. Section 4 proposed the PVP simulation result, the validation of the proposed approach is provided in Section 5. Finally, Section 6 gives the conclusion.

2. PVP model

For convenience and completeness of the paper we will explain hereafter the PVP modelling. A photovoltaic cell is basically a p–n semiconductor junction diode which converts solar light energy into electricity. Its equivalent circuit is shown by Fig. 1.

A PVP is composed of n_p parallel modules each one including n_s photovoltaic cell serial connected. The fundamental equation for PVP model is given by Eq. (1) [4,17].

$$I = n_p I_{ph} - n_p I_{rs} \left[\exp \left(\frac{q(V_g + IR_s)}{kTAn_s} \right) - 1 \right] - \frac{V_g + IR_s}{R_{sh}} \quad (1)$$

where I and V_g are respectively the PVP output current and voltage, I_{ph} the generated photocurrent (A), R_s and R_{sh} respectively the serial and the parallel resistances of the PV cell (Ω), q is the electron charge, k the Boltzmann's constant, A is the p–n junction ideality factor, T is the cell temperature and I_{rs} is the cell reverse saturation current. I_{rs} is related to the temperature T as follows:

$$I_{rs} = I_{rr} \left[\frac{T}{T_r} \right]^3 \exp \left(\frac{qE_G}{kqA} \left[\frac{1}{T_r} - \frac{1}{T} \right] \right) \quad (2)$$

where T_r is the cell reference temperature, I_{rr} is the reverse saturation current at T_r and E_G is the band-gap energy of the semiconductor. Similarly, the photocurrent I_{ph} depends on the solar

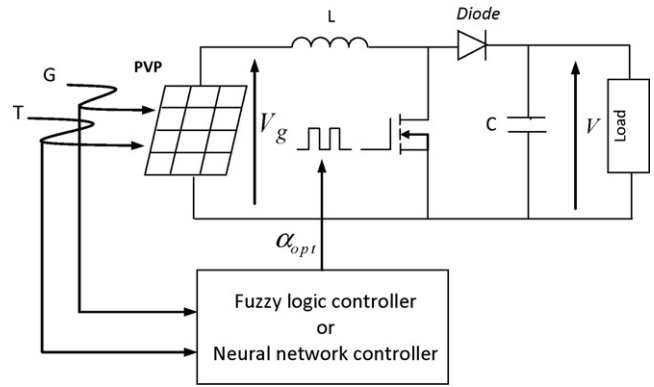


Fig. 2. System configuration.

radiation and the cell temperature as follows:

$$I_{ph} = [I_{sc} + k_i(T - T_r)] \frac{G}{1000} \quad (3)$$

where I_{sc} is the PVP short-circuit current at reference temperature and radiation, G is the solar radiation and k_i the temperature coefficient for short-circuit current. The PVP power is then calculated as

$$P = IV_g \quad (4)$$

3. Methodology

Fig. 2 shows the MPPT connecting the PVP module to the dc load. The MPPT consists of boost dc–dc inverter with the output filter and the control system (FL or NN controllers). The MPPT drives the operating point of the PVP to the P_{max} detected by the control system.

The control unit switches the power transistor ON and OFF to carry out the P_{max} from the PVP. When the transistor is switched ON, the current in the boost inductor increases linearly, so the diode is in the OFF state. However, when the transistor is switched off, the energy stored in the inductor is released through the diode to the load. The pulsating current produced by the switching action is smoothed by the capacitive filter and a dc voltage is provided to the load.

The boost converter transfer function is obtained by considering its steady state operation as follows:

$$\frac{V}{V_g} = \frac{1}{1 - \alpha} \quad (5)$$

where α is the duty cycle given by the control unit, V is the output voltage and V_g is the output PVP voltage.

Our work consists to command a boost converter to obtain the MPPT directly from the climatic data such as G and T . Our approach is to build a FL and NN MPPT controllers based on a practice data base measured by a PVP, a variable resistor, an acquisition chain, a temperature sensor and solar radiation sensor.

To release the relationships $I=f(V)$ and $P=f(V)$ of the panel, we proceed through varying rapidly the resistance for fixed G and T . We start with a very large resistance value ($\sim M\Omega$) which corresponds to an open circuit voltage V_{oc} and to a zero current until we reach a resistance of 0Ω corresponding to the short-circuit current I_{sc} and zero voltage.

Next, observing the graphical realizations $P=f(V)$ and $I=f(V)$, the maximum power points are read directly from the first curve. V_{opt} is the X-coordinate of P_{max} . The optimal current I_{opt} is then obtained from the curve $I=f(V)$.

Finally, α_{opt} is deduced from Eq. (5) when letting $V_g = V_{opt}$ and $V = 24V$.

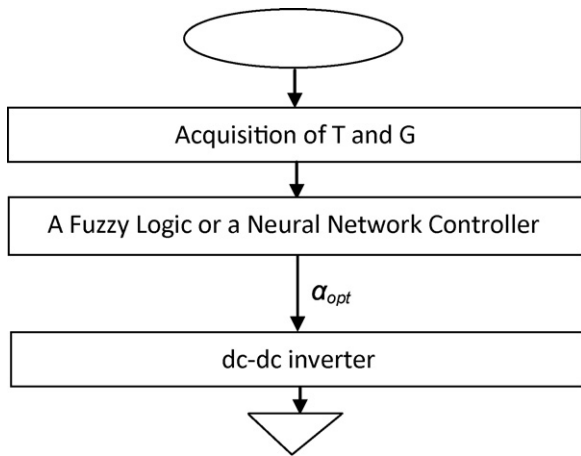


Fig. 3. Algorithm steps.

The procedure explained above is then repeated to yield a data basis $(G, T, P_{max}, \alpha_{opt})$ to be used as a building and validation for the FL and NN controllers.

Contrarily to some existing approaches [3,4], the computation of the parameter α_{opt} in the present work is based on a step-by-step procedure. Next, a building step which consists in testing the relationship $\alpha_{opt} = f(T, G)$ on a FL and a NN controllers basis is provided. We use as inputs the values of T, G and α_{opt} furnished in step one. The last step prepares for possible evaluation or prediction of the parameter α_{opt} for given T and G without cross-passing by step one. Fig. 3 hereafter summarizes these steps.

3.1. Fuzzy logic MPPT controller

Fuzzy logic is one of the most powerful control methods. It is known by multi-rules-based resolution and multivariable's consideration [9]. Compared to other methods such as neural networks and genetic algorithms, it provides fast results using the expert knowledge and measured data base. Hence, fuzzy logic method has been selected as a management tool for the present system. This selection is judicious considering that it fulfills well the system requirements. Since the MPPT controller approach uses fuzzy logic, its algorithm is based on three steps: the knowledge base of the expert, the fuzzification, the inference diagram and the defuzzification [9,18].

3.1.1. The knowledge base of the expert

The approach handles a multi-criteria resolution for which three fuzzy partitions are judged necessary:

- According to solar radiation: the fuzzy partition of solar radiation is composed of $N_s = 4$ fuzzy subsets. $A_i = (\text{Small, Means, Large, Very large})$ is the i th fuzzy subset, $i = \{1, 2, 3, 4\}$. These subsets cover the fuzzy domain $x = [0, 1200]$ and verify $\forall x_1 = G_i \in x, \sum_{i=1}^{N_s} \mu_{A_i}(x) = 1$, where G_i is the solar radiation value and μ_{A_i} is the membership function.
- According to PV cell temperature: the fuzzy partition of PV cell temperature is composed of $N_s = 4$ fuzzy subsets. $B_j = (\text{Small, Means, Large, Very large})$ is the j th fuzzy subset, $j = \{1, 2, 3, 4\}$. These subsets cover the fuzzy domain $y = [0, 1200]$ and verify $\forall y_j = T_j \in y, \sum_{i=1}^{N_s} \mu_{B_j}(y) = 1$, where T_j is the solar radiation value and μ_{B_j} is the membership function.
- According to optimum duty cycle α_{opt} : the fuzzy partition of solar radiation is composed of $N_s = 4$ fuzzy subsets. $C_k = (\text{Small, Means, Large, Very large})$ is the k th fuzzy subset, $k = \{1, 2, 3, 4\}$. These subsets cover the fuzzy domain $z = [0, 1200]$

Table 1 Control rules.

T [°C]	G [W/m ²]			
	Small	Means	Large	Very Large
Means	Means	Means	Large	Small
Large	Means	Large	Large	Very Large
Very Large	Small	Means	Very Large	Very Large

and verify $\forall z_i = \alpha_{opt k} \in Z, \sum_{i=1}^{N_s} \mu_{C_k}(z) = 1$, where $\alpha_{opt k}$ is the solar radiation value and μ_{C_k} is the membership function.

The control rules are indicated in Table 1 with radiation G and temperature T as the inputs and duty Cycle α_{opt} as the output. These two input variables and the control action duty Cycle α_{opt} for the tracking of the maximum power point.

3.1.2. The fuzzification

The determined fuzzy partition leads to the calculation of the membership functions μ_{A_i}, μ_{B_j} and μ_{C_k} considering the symmetric triangular type (Fig. 4). These membership functions are to be expressed as

$$\mu_{A_i}(x_{0i}) = \begin{cases} 1 - \frac{|x - x_{0i}|}{\epsilon_{x_{0i}}} & \text{if } |x - x_{0i}| \leq \epsilon_{x_{0i}} \\ 0 & \text{otherwise} \end{cases}$$

for the solar radiation G (6)

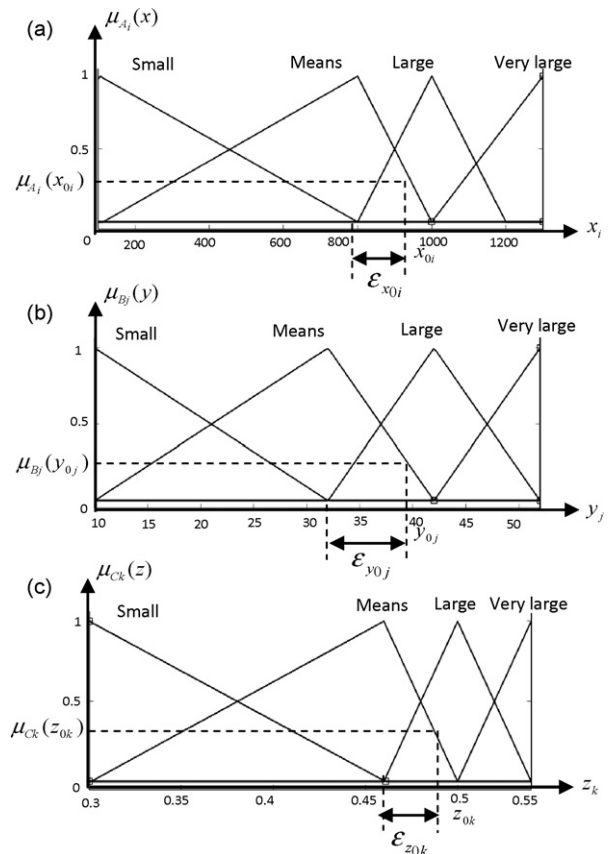


Fig. 4. Fuzzy logic membership function of (a) solar radiation, (b) PV cell temperature, and (c) optimum duty cycle.

$$\mu_{B_j}(y_{0j}) = \begin{cases} 1 - \frac{|y - y_{0j}|}{\varepsilon_{y_{0j}}} & \text{if } |y - y_{0j}| \leq \varepsilon_{y_{0j}} \\ 0 & \text{otherwise} \end{cases}$$

for the PV cell temperature T (7)

$$\mu_{C_k}(z_{0k}) = \begin{cases} 1 - \frac{|z - z_{0k}|}{\varepsilon_{z_{0k}}} & \text{if } |z - z_{0k}| \leq \varepsilon_{z_{0k}} \\ 0 & \text{otherwise} \end{cases}$$

for the optimum duty cycle α_{opt} (8)

3.1.3. Inference diagram

By means of the obtained membership function, a rule base is established, according to Mamdani [1], using the general rule format:

$$R_{ijk} \text{ if } (x_i \text{ is } A_i \text{ and } y_j \text{ is } B_j) \text{ then } z_k \text{ is } C_k \quad (9)$$

where x_i is the solar radiation (G) vector and A_i its linguistic value, y_j the PV cell temperature (T) and B_j its linguistic value, z_k the optimum duty cycle and C_k its linguistic value.

Since the decision is taken (which case to consider), Eq. (9) is therefore computed for $i = 1, 2, 3, 4; j = 1, 2, 3, 4$; to generate a rules base composed of $4 \times 4 = 16$ rules. The rules' aggregations are given by computing the minimum norm conjunction implication of fuzzy subset of the optimum duty cycle α_{opt} .

$$\mu_{C'_k} = \min(w_k, \mu_{C_k}) \quad (10)$$

$$\mu_{C'_{k+1}} = \min(w_{k+1}, \mu_{C_{k+1}}) \quad (11)$$

where w_k is the minimum norm fuzzy conjunction between the i th fuzzy subset of the solar radiation and j th fuzzy subset of the PV cell temperature:

$$w_k = \min(\mu_{A_i}, \mu_{B_j}) \quad (12)$$

and w_{k+1} is the minimum norm fuzzy conjunction between the $(i + 1)$ th fuzzy subset of the G and $(j + 1)$ th fuzzy subset of the T .

$$w_{k+1} = \min(\mu_{A_{i+1}}, \mu_{B_{j+1}}) \quad (13)$$

Using the maximum t-conorm rule aggregation, the membership function for an operating point of the option α_{opt} is given by

$$\mu_C = \max(\mu_{C'_k}, \mu_{C'_{k+1}}) \quad (14)$$

3.1.4. Defuzzification

Since the rules are aggregated, the defuzzification consists in calculating the real value z_{0k} of α_{opt} using the centroid method (z_{0k} is the centre of μ_C):

$$z_{0k} = \frac{\int_0^1 z_k \mu_C dz_k}{\int_0^1 \mu_C dz_k} \quad (15)$$

3.1.5. The management algorithm

- Acquire:** G_i, T_j {read G and T }
- Fuzzification:** Compute μ_{A_i}, μ_{B_j} and μ_{C_k} {the membership function}
- Inference diagram:** Compute R_{ijk} : if $(x_i \text{ is } A_i \text{ and } y_j \text{ is } B_j)$ then z_k is C_k {the rules base}; Calculate μ_C {the membership functions of the operating points}
- Defuzzification:** Compute z_{0k} the centers of μ_C {using the centroid method}

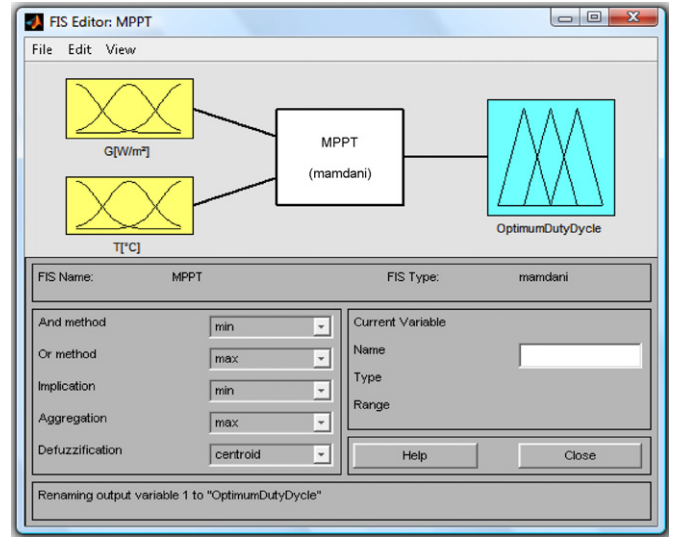


Fig. 5. Matlab windows of the fuzzy logic Controller.

3.1.6. The Matlab windows

Fig. 5 presents the fuzzy logic Matlab simulink windows which composed the MPPT controller, his inputs T and G , her output α_{opt} and the different parameters of the fuzzification, implication the aggregation and the defuzzification.

3.2. Neural network MPPT controller

NN can generally be thought of as black box devices that accept inputs and produce outputs. The neural systems function as parallel distributed computing networks, the MPPT controller approach uses neural network are presented in the paper [15,16].

The NN controller is used to estimate the optimum duty cycle α_{opt} which corresponds to P_{max} at any given solar radiation G and PV cell temperature T . Fig. 6 shows the NN controller.

In our application, we elaborated a recursive multi-layer network where calculations occur only in one direction conducted from inputs to outputs. As shown in Fig. 6, the NN controller consists of three layers. The input layer is composed of two nodes in inputs that are; the PV cell temperature T and the solar radiation G . The hidden layer composed of seven nodes whose function of activation is sigmoid. The output layer is composed of one node that is the optimum duty cycle α_{opt} which corresponds to the P_{max} whose function of activation is of linear type.

Here N_h designates the number of hidden neurons. The connection weight values and the thresholds of the NN are selected randomly at the starting of the training process and then dur-

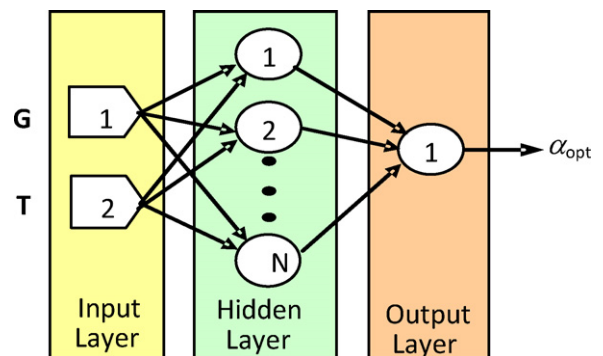


Fig. 6. The neural network architecture.

Table 2
Electrical characteristics of the 50 W single-crystalline photovoltaic module SM50-H.

Parameter (at STC)	Abbreviation	Value
Band-gap energy	E_G	1.12 eV
Ideal factor	A	1.5
Maximum power	P_{max}	50 Wp
Rated current	I_{MPP}	3.15 A
Rated voltage	V_{MPP}	15.9 V
Short-circuit current	I_{sc}	3.35 A
Open circuit voltage	V_{oc}	19.8 V
Temperature coefficient of I_{sc}	k_i	1.2 mA/°C
Normal operating cell temperature	NOCT	45 ± 2 °C
Cell serial modules	n_s	33

ing training they are fixed so as to make minimum square error between estimated and training data. A great number of the processes of training are available. In our case, we used the retro-propagation method which is the most known and the most used. The training algorithm consists of minimizing the total error E defined by the following equation [11,18]:

$$E = \frac{1}{2} \sum (O_n - t_n)^2 \tag{16}$$

where O_n is the n th measured output read by the network and t_n is the n th target (the estimated output). Hence each input/output pair constitutes a training sample. The retro-propagation algorithm calculates the error E and distributes it back from output towards input neurons through the hidden neurons using following formula [12]:

$$\Delta w_n = \delta \Delta w_{n-1} - \eta \frac{\partial E}{\partial w} \tag{17}$$

where w is the weight between any two neurons, Δw_n and Δw_{n-1} are the changes of these weights for n and $n - 1$ iterations, δ is the speed term and η is the training rate. The training rate determines the size of the changes of the weights caused by the effect of the total error. The speed term avoids the oscillations of weight during the training iterations and also accelerates the training on error surface. The selected number of neurons in the hidden layer determines the training degree. This number is calculated by the empirical following formula [9]:

$$N_h = \frac{1}{2}(N_I + N_O) + \sqrt{N_E} \tag{18}$$

where N_I is the number of input neurons, N_O is the number of output neurons and N_E is the size of training sample.

For the size of the training sample of the neural network is $N_E = 37$. These parameters yield, using Eq. (8), a number of nodes in the hidden layer is seven nodes. We just recall here that the exact value deduced from Eq. (8) is $N_h = 7.58$. So, the nearest values are 7 and 8. A comparison between them yields good results for a choice of $N_h = 7$.

4. PVP simulation result

Based on the fact that PVP outputs depend on solar radiation and ambient temperature as in Eqs. (1) and (4), their simulations deliver two types of curves.

For this goal we use two parallel Siemens SM50-H PV modules. The parameters of the developed model are given in Table 2 hereafter. Such parameters are considered at the Standard Test Condition (STC): 1 kW/m² (1 Sun) at spectral distribution of AM 1.5 and cell temperature of 25 °C.

Furthermore, using the derivative procedure of each PVP power curve, a new maximum power characteristic is extracted to indicate the optimal functioning points for the PVP (I_{opt} , V_{opt}) for different

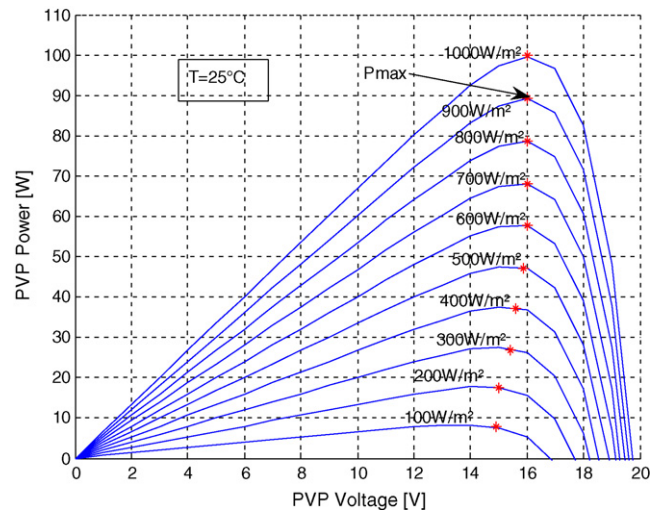


Fig. 7. Simulated P/V characteristics of PVP model at constant temperature $T = 25$ °C.

solar radiation and ambient temperature. Figs. 7 and 8 plot $P=f(V)$ and $I=f(V)$ curves respectively for different solar radiation G and with constant temperature $T = 25$ °C. Figs. 9 and 10 present the same parameters curves for different temperature T but with constant solar radiation $G = 100$ W/m².

As it is shown in Figs. 7 and 8, the current, due to the cutoff circuit is positively varying with solar radiation. However, the voltage in the open circuit remains quasi constant. Furthermore, maximum power points are situated around a critical value of 16 V. The charge regulator, the MPPT, will not be perturbed enough by the solar radiation when searching the maximum power points.

Figs. 9 and 10 show that the affect of temperature is slightly significant, and it needs important choice in panel and systems conception. The temperature has a negligible effect on the cutoff circuit current. However, the open circuit voltage decays rapidly as the temperature increases.

5. System experimental validation

In this section, experimental tests are provided based on theoretical concepts previously exposed. The measures were realized on the PVP module previously modelled. Hence, since the model is established and validated, it is used to compute, for a given tem-

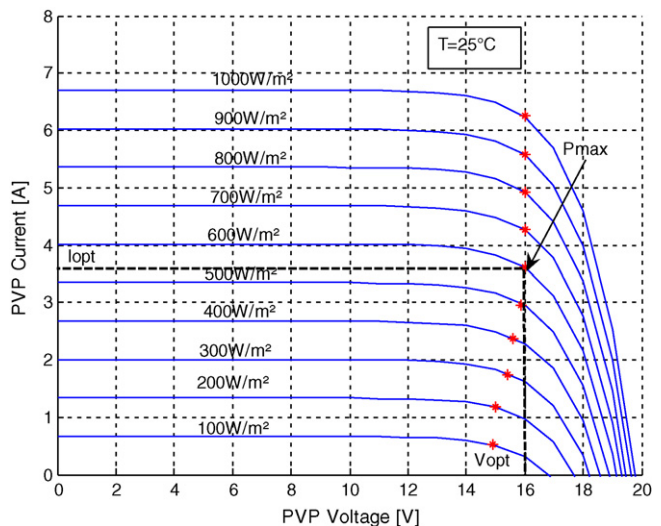


Fig. 8. Simulated I/V characteristics of PVP model at constant temperature $T = 25$ °C.

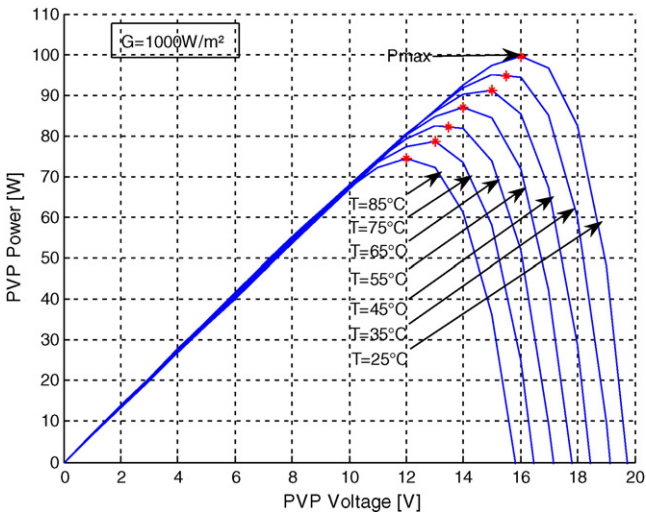


Fig. 9. Simulated P/V characteristics of the PVP model at constant solar radiation 1000 W/m^2 .

perature and irradiation, the duty cycle which controls the dc–dc inverter to track the maximum power.

The model of test composing of two parallels connected photovoltaic modules SM50-H, a variable resistor, an acquisition chain, a temperature sensor and solar radiation sensor (Fig. 11). With this test model we proceed through varying rapidly the resistance for G and T fixed. We start with a very large resistance value ($\sim\text{M}\Omega$) which corresponds to an open circuit voltage V_{oc} and to a zero current until reaching a resistance of $0\ \Omega$ corresponding to the short-circuit current I_{sc} and zero voltage. The procedure explained above is then repeated to yield a data basis ($G, T, P_{max}, \alpha_{opt}$) to be used as a building and validation for the FL and NN controller.

The FL and the NN algorithms have been implemented in the system shown in Fig. 1. A FL and a NN models were established on the basis of a data base of measures taken in advance on the system (see Table 3). This data base contains different values of PV cell temperature T , solar radiation G , and measured duty cycle using the test model Fig. 11. The obtained FL and a NN models are consequently used during function to determine the optimum duty cycle α_{opt} of the PWM signal which controls the dc–dc inverter so as to track the MP from the PVP.

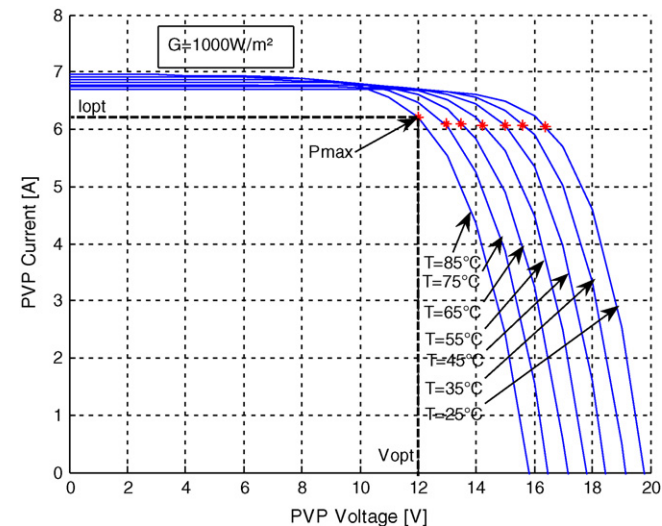


Fig. 10. Simulated I/V characteristics of the PVP model at constant solar radiation 1000 W/m^2 .

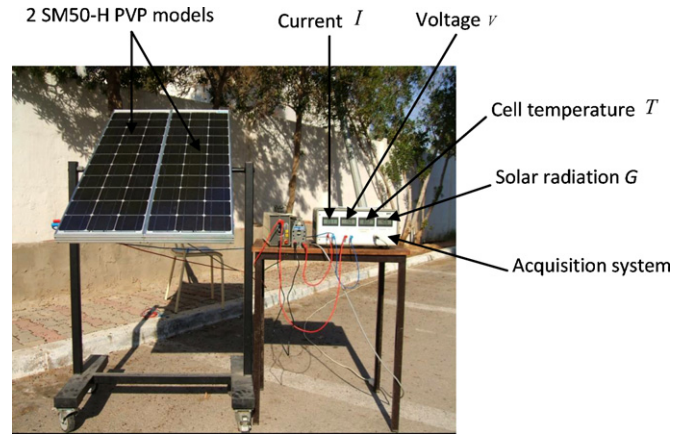


Fig. 11. The model of test.

Fig. 12 shows the measured and the FL and the NN estimated optimum duty cycle α_{opt} for different solar radiations. It is shown that the estimated curves of the FL method and the NN method fit well the measured one.

Next, Fig. 13 shows the measured and the estimated P_{max} values for different climate data G and T .

It is clear that the estimated and the measured powers equally follow the climatic parameters (T, G) even for a fast variation of the solar radiation.

As it is shown in Figs. 12 and 13 the measured and estimated curves fit well. This fact is also confirmed by the following table (Table 4) which gives the relative errors between the estimated and the experimental series.

FL gives power with minimum total error compared to NN method. This shows that the best method is FL among the NN.

From these figures, it is clear that the FL and NN controllers accurately estimate the MPPT at any solar radiation and PVP cell temperature.

The performance of the MPPT can be detected according to the efficiency [16,19]. The efficiency calculated by the following equation:

$$\text{Efficiency} = \left(1 - \frac{\text{Measured } P_{max} - \text{Estimated } P_{max}}{\text{Measured } P_{max}} \right) \times 100 \quad (19)$$

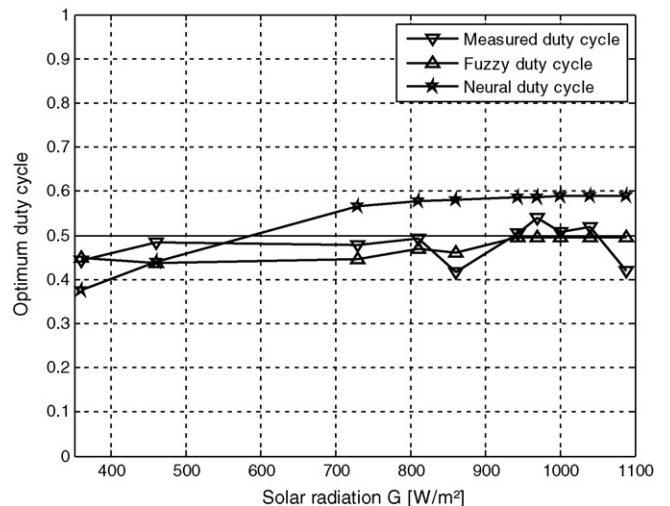


Fig. 12. Measured and estimated duty cycle.

Table 3
Data base.

G [W/m ²]	T [°C]	Measured	Fuzzy α_{opt}	Neural α_{opt}	Measured P_{max}	Fuzzy P_{max}	Neural P_{max}
360	37.3	0.4489	0.4417	0.3756	32.0130	31.6543	34.6443
460	36.7	0.4381	0.4833	0.4400	38.1818	41.2485	41.1256
730	36	0.4447	0.4792	0.5650	61.1567	65.0052	51.2251
810	41	0.4683	0.4938	0.5770	66.1623	69.4059	55.3830
861	36	0.46	0.4167	0.5818	80.3150	74.7367	58.1004
943	44	0.495	0.5042	0.5862	75.5789	76.9609	63.1513
970	44	0.495	0.5396	0.5871	72.2440	79.1683	64.8192
1000	47	0.4952	0.5083	0.5879	81.6837	79.5896	66.7674
1040	44	0.495	0.5188	0.5887	80.9350	84.8913	69.2297
1088	39.7	0.4951	0.4208	0.5894	101.2237	88.6506	72.1910

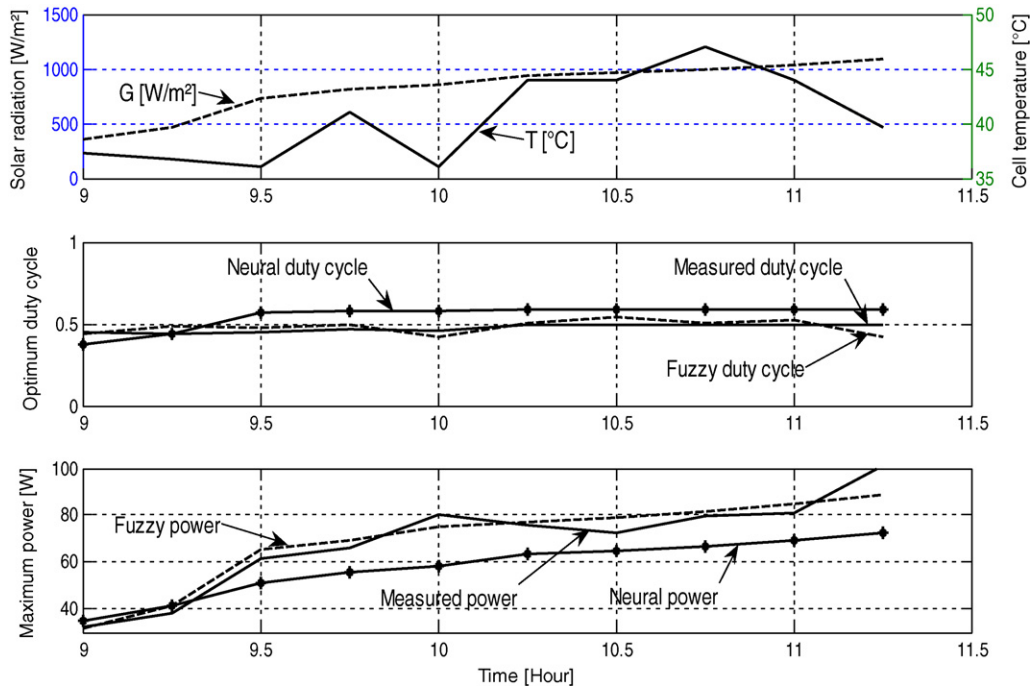


Fig. 13. System validation results.

The efficiency of FL and NN controllers are shown in Fig. 14. The figure shows that the FL controller can generate up to 99% of the actual maximum power and the NN controller can generate up to 92% of it.

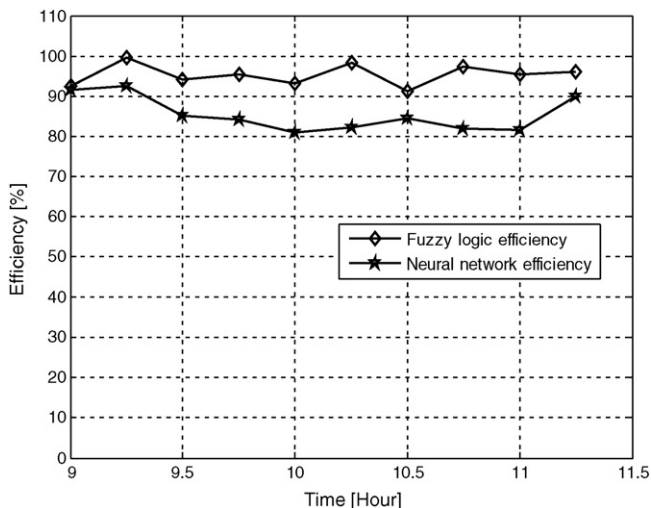


Fig. 14. Efficiency of FL and NN MPPT.

Table 4

The normalized errors of measured and predicted values.

Method	Optimum duty cycle error	Maximum power P_{max} error
Fuzzy logic	2.7087	0.0761
Neural network	17.1539	0.5381

6. Conclusion

Two new MPPT methods based on the FL in the first and on the NN in the second were proposed and investigated. FL and NN can model dynamical complex systems that change with time following non-linear laws. These proposed algorithms in FL and NN consist in commanding a boost dc–dc inverter to obtain the MPPT directly from the climate data solar radiation and PV cell temperature. In addition these two MPPT give a simplified system and low cost to implement it. The results of the experiment have shown that the MPPT controller by using FL has provided more power than the NN one.

References

[1] N.A. Ahmed, M. Miyatake, A novel maximum power point tracking for photovoltaic applications under partially shaded insolation conditions, *Electric Power Systems Research* 78 (2008) 777–784.

- [2] V. Salas, E. Olias, A. Barrado, A. Lazaro, Review of the maximum power point tracking algorithms for stand-alone photovoltaic systems, *Solar Energy Materials & Solar Cells* 90 (2006) 1555–1578.
- [3] W. Xiao, W.G. Dunford, P.R. Palmer, A. Capel, Application of centered differentiation and steepest descent to maximum power point tracking, *IEEE Transactions on Industrial Electronics* 54 (2007) 2539–2549.
- [4] G.J. Yu, Y.S. Jung, J.Y. Choi, G.S. Kim, A novel two-mode MPPT control algorithm based on comparative study of existing algorithms, *Solar Energy* 76 (2004) 455–463.
- [5] S. Jain, V. Agarwal, New current control based MPPT technique for single stage grid connected PV systems, *Energy Conversion and Management* 48 (2007) 625–644.
- [6] S. Kim, Robust maximum power point tracker using sliding mode controller for the three-phase grid-connected photovoltaic system, *Solar Energy* 81 (2007) 405–414.
- [7] H. Chih-Lyang, C. Li-Jui, Y. Yuan-Sheng, Network-based fuzzy decentralized sliding-mode control for car-like mobile robots, *IEEE Transactions on Industrial Electronics* 54 (2007) 574–585.
- [8] T.A. Venelinov, C.G. Leonardo, G. Vincenzo, C. Francesco, K. Okyay, Sliding mode neuro-adaptive control of electric drives, *IEEE Transactions on Industrial Electronics* 54 (2007) 671–679.
- [9] Ch. Ben Salah, M. Chaaben, M. Ben Ammar, Multi-criteria fuzzy algorithm for energy management of a domestic photovoltaic panel, *Renewable Energy* 33 (2008) 993–1001.
- [10] S.A. Kalogirou, Artificial neural networks in renewable energy systems applications: a review, *Renewable and Sustainable Energy Reviews* 5 (2001) 373–401.
- [11] B. Leger, J.B. Lopez-Velasco, J.M. Emidio, Thermal flux characterization of multi-holed plates using neural networks: application to combustion chamber walls, *International Journal of Thermal Sciences* 41 (2002) 1089–1100.
- [12] F. Moutarde, Introduction aux réseaux de neurones, Ecole des Mines de Paris Avril, 2007.
- [13] N. Patcharaprakiti, S. Premrudeepreechacharn, Y. Sriuthaisiriwong, Maximum power point tracking using adaptive fuzzy logic control for grid-connected photovoltaic system, *Renewable Energy* 30 (2005) 1771–1788.
- [14] N.A. Gounden, S.A. Peter, H. Nallandula, S. Krithiga, Fuzzy logic controller with MPPT using line-commutated inverter for three-phase grid-connected photovoltaic system, *Renewable Energy* 34 (2009) 909–915.
- [15] A.B.G. Bahgat, N.H. Helwa, G.E. Ahamd, E.T. El Shenawy, Estimation of the maximum power and normal operating power of a photovoltaic module by neural networks, *Renewable Energy* 29 (2004) 443–457.
- [16] A.B.G. Bahgat, N.H. Helwa, G.E. Ahamd, E.T. El Shenawy, Maximum power tracking controller for PV systems using neural networks, *Renewable Energy* 30 (2005) 1257–1268.
- [17] T. Kawamura, K. Harada, Y. Ishihara, T. Todaka, T. Oshiro, H. Nakamura, M. Imataki, Analysis of MPPT characteristics in photovoltaic power system, *Solar Energy Materials and Solar Cells* 47 (1997) 155–165.
- [18] C. Larbes, S.M.A. Cheikh, T. Obeidi, A. Zerguerras, Genetic algorithms optimized fuzzy logic control for the maximum power point tracking in photovoltaic system, *Renewable Energy* 34 (2009) 2093–2100.
- [19] A.D. Karlis, T.L. Kottas, Y.S. Boutalis, A novel maximum power point tracking method for PV systems using fuzzy cognitive networks (FCN), *Electric Power Systems Research* 78 (2007) 315–327.